Review article

MXene-based flexible electronic materials for wound infection detection and treatment

Check for updates
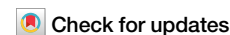
Yanling Hu[1,2], Fangfang Wang[3], Hui Ye[1], Jingai Jiang[3], Shengke Li[1], Baoying Dai[1], Jiahui Li [1], Jun Yang [1], Xuejiao Song[3], Junjie Zhang[4], Yannan Xie [1] ✉, Li Gao[1] ✉ & Dongliang Yang [3] ✉

Wound infection is a worldwide health issue that not only brings large detrimental effects to people's physical and mental health, but also causes substantial economic burdens to society. By using traditional surgical debridement and antibiotic therapy, patients generally suffer more pain and are at risk of recurring infections. Thus, the development of non-antibiotic treatment methods is desperately needed. Currently, the emerging of flexible wound dressings with physiological signal detection, inactivated infectious pathogen, and wound-healing promoting properties has exhibited immense potential for the treatment of infected wound. Among various dressings, MXene-based flexible electronic materials as wound dressings with special electroactive, mechanical, photophysical, and biological performances possess a broad application prospect in healthcare. In this review, the challenges of infected wound management are introduced. Next, the types of MXene-based flexible materials and wound infection features are outlined. Then the recent advance of MXene-based flexible materials for infected wound detection and treatment is summarized. Lastly, the predicaments, prospects, and future directions of MXene-based flexible materials for infected wound management are discussed.

Bacterial infections not only hinder wound healing progress, but also worsen wounds which may lead to amputation, and even threaten a person's life, which have long aroused people's great attention[1]. In general, the skin on the body surface plays a vital role in preventing bacterial invasion and external physical damage[2]. However, once the function and integrity of skin is disrupted, a wound will form. The wound effluent may create a favorable environment for bacterial propagation[3]. In some special circumstances, the bacteria that locate in the wound will proliferate and form a functional biofilm with three dimensional structure[4]. Due to the presence of biofilm extracellular matrix, the antibacterial agents cannot encounter bacteria that are located inside the biofilm, further causing persistent infection and inflammation which eventually resulting in the refractory wound infections[5,6]. For example, there are 2 to 4.5 million chronic wound patients in the United States alone, and these patients cost $20 billion dollar annually[7]. Unfortunately, this expenditure will increase as the aging population and the number of diabetic patients increases[8]. Thus, developing therapeutics that can effectively treat infected wounds is important to improve patients' life quality and reduce the overall medical expenditure.

In the realm of clinical wound treatment, traditional wound dressings present a range of challenges, including the need for frequent replacement that can result in wound re-injury and secondary infections. Moreover, these traditional dressings exhibit deficiencies such as subpar mechanical properties, absence of biological activity, limited oxygen permeability, inadequate adhesion and etc. Consequently, traditional wound dressings fall short of providing sufficient protection for the wound and promoting expedited wound healing[9,10]. Currently, flexible material-based dressings have a strong practical application prospect in wound treatment[11]. After administration, the flexible materials will be in close contact with the wound. Thus, its mechanical properties and biological activity are extremely vital to wound treatment. For example, flexible materials without inducing biological toxic side effects (e.g.,

[1]State Key Laboratory of Organic Electronics and Information Displays & Jiangsu Key Laboratory for Biosensors, Institute of Advanced Materials (IAM), Nanjing University of Posts & Telecommunications, Nanjing, China. [2]College of Life and Health, Nanjing Polytechnic Institute, Nanjing, China. [3]Key Laboratory of Flexible Electronics (KLOFE) and Institute of Advanced Materials (IAM), School of Physical and Mathematical Sciences, Nanjing Tech University (NanjingTech), Nanjing, China. [4]School of Fundamental Sciences, Bengbu Medical University, Bengbu, PR China. ✉e-mail: iamynxie@njupt.edu.cn; iamlgao@njupt.edu.cn; yangdl1023@njtech.edu.cn

1

cytotoxic, or immune reactions) is the most basic requirement. In addition, the materials should have antibacterial and anti-inflammatory activities, and the properties of promoting cell proliferation and migration, angiogenesis, and collagen deposition, are conducive to rapid healing of infected wound[12]. Aside from regulating the biological activity of wound repair cells, wound healing can also be accelerated by reshaping the external environment of the wound[13]. Previous results confirm that a moist and hyperoxic environment can facilitate wound healing[14,15]. Thus, innovative wound dressings with appropriate biological activities and physicochemical properties (e.g., mechanical strength, moisture retention, breathability, flexibility, etc.) are favorable[16]. Compared with conventional flexible wound dressings, MXene-based flexible therapeutics show high electrical conductivity, photothermal conversion ability, rich surface chemistry, and acceptable biocompatibility, which can remove infectious pathogens by photothermal therapy or nano-knife effect[17], and provide a physical protective barrier for the wound[18]; meanwhile, it is also conducive to reconstruct the endogenous electric field of wound, further boosting wound closure[19].

Wound healing is a complex and dynamic process[20]. To enhance the therapeutic effect of chronic infected wounds, therapeutic agents are better able to perform different biological activities at different stages[21]. Therefore, the development of responsive wound dressings is extremely important for wound treatment. At present, some important breakthroughs have been made in wound dressing with infected microenvironment (e.g., acidity, enzyme, temperature, etc.) and physical signals (e.g., light, ultrasound, magnetism, and etc.) stimulus-response performance[22,23]. However, most wound dressings cannot reflect wound healing state and wound infection information, which limits the personalized treatment[24]. Currently, traditional detection strategies for wound infection are highly dependent on biochemical pathological analysis and personal experience, which may lead to delayed diagnosis and misdiagnosis, respectively[25]. Hence, the integration of wound monitoring and treatment performances into wound dressings are urgently desirable. By using these flexible dressings, infected wound can be treated more effectively, which offers an innovative therapeutic method in the treatment of infected wound.

With the deepening of research on infected wound, a series of markers that relate to wound status have been discovered. Several results confirm that the analysis of physiochemical signals (e.g., pH, temperature, enzyme, glucose, uric acid, etc.) can be used to estimate the condition of an infected wound[26–28]. In the last decades, many light and electrochemical-based sensors have been developed for the detection of infected wound[29]. Among them, flexible and wearable sensors have obtained considerable attention as it can offer real-time biological information about infected wounds in situ. Moreover, these sensors can be integrated with controlled drug delivery systems and wireless transmitters to enable real-time monitoring of the healing process of infected wounds and personalized treatment.

To improve the electrical, mechanical, and sensing properties of wearable wound dressing, many organic or inorganic materials have been introduced during the synthesis of flexible materials[30]. For example, compared to graphene, MXene exhibits a lower modulus, but its bending stiffness surpasses that of graphene significantly. Consequently, MXene offers a more balanced mechanical profile, making it highly suitable for flexible material[31]. In the wound infection treatment, MXene outshines carbon nanotubes due to its physical antibacterial properties attributed to the nanoknife effect[17]. In addition, MXene with superior conductivity, large surface areas, adjustable structural crystallinity, and hydrophilicity, have been extensively investigated in the field of flexible electronics[32]. So far several reviews have made systematic summaries of MXene application in wearable flexible electronics[33–35]. However, MXene-based flexible materials as wound dressing for infected wound management have not been summarized yet.

In this review, the crisis of infected wound management and flexible wound dressing are introduced first. Then the types of MXene-based flexible materials are briefly outlined. Subsequently, MXene-based flexible materials for the detection of infected wound markers and the treatment of infected wounds are systematically summarized (Fig. 1). Lastly, the bottlenecks of MXene-based flexible materials in the management of infected wounds and

their future opportunities are discussed. We hope that this review offers some references to tailor and synthesize MXene-based flexible material for infected wound treatment.

MXene-integrated flexible materials

Due to its physical properties, MXenes have attracted much attention in biomedical fields (e.g., antibacterial, tumor therapy, flexible electronics, sensing, etc.)[17,35,36]. The bioinertness, hydrophilicity, conductivity, photosensitivity, and photothermal conversion activity of MXenes makes it a common material in the field of healthcare. For example, in the infected wound treatment, MXene-based flexible materials are favorable because it is easy to use. According to the application requirements of different scenarios, a variety of MXene-based flexible materials with different mechanical and biological activities have been developed for the management of infected wounds. At present, these flexible materials mainly include plastic, fabric, rubber, aerogel, hydrogel and etc[37]. The research shows that different kinds of flexible materials have their own characteristics. For example, hydrogels with excellent biocompatibility and similar mechanical properties to human tissue have been widely employed in the tissue regeneration, tumor treatment, drug delivery, and wound dressing[38,39]. The integration of MXene and hydrogel could not only significantly improve the stability of MXene, but also endow the hydrogel with high conductivity[40]. In addition, by introducing bioactive substances, MXene-based hydrogels can used as wound theranostics[41]. Another flexible conductive fabric can be facilely and rapidly prepared by direct spraying MXene material. MXene-integrated fabrics with breathability, flexibility, lightweight, resiliency, and conductivity, are also favorable for wound dressing. Compared with hydrogel and fabric, plastics and rubbers with a strong mechanical performance are important flexible substrate material[42]. Thus, scientists and healthcare workers can choose appropriate flexible substrate to realize the detection and treatment of wound infections according to their demands.

Infected wound features

Clinical studies demonstrate that the interaction between the pathogens and host will create an infected wound microenvironment[43]. For example, the
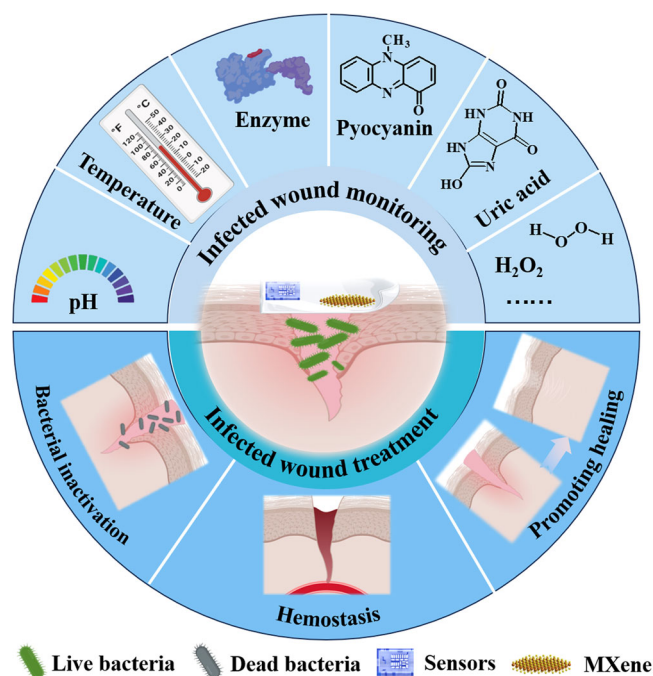

Fig. 1 | MXene-based flexible materials for infected wound monitoring and treatment. The infection characteristics for infected wound detection include abnormal pH, temperature, enzymes, toxins, and oxidative stress. The wound treatment processes include bacterial removal, hemostasis, wound healing.

Table 1 | Summary of MXene-based flexible sensors

Flexible sensor	Biomarker	Method	Signal	Ref
FLEX-AI wearable sensor	H^+	Electrochemical	Voltage	58
Cu NPs@Cu-MOF/Ti$_3$C$_2$Tx-modified flexible screen-printed electrode	H_2O_2	Electrochemical	Current	62
Mn$_3$(PO$_4$)$_2$/MXene/PE film electrode	Superoxide anion	electrochemical	Current	68
Au-Pd/Ti$_3$C$_2$Tx/laser scribed porous graphene flexible sensor	Uric acid	Electrochemical	Current	73
MXene/AuNPs/peptides electrode	Sortase A	Electrochemical	Current	78
Uricase (UOx)-modified LGG-MXene	Uric acid	Electrochemical	Current	80
NPC@MXene/Au electrode	Glucose	Electrochemical	Current	81

pH value in the infected wound is acidic due to the bacteria that colonize the wound undergo anaerobic metabolism. During bacterial growth, many metabolites (e.g., lactic acid and uric acid, etc.)[26] and virulence factors (e.g., membrane proteins, polysaccharide capsules, secretory proteins, toxins, etc.)[44] will be produced and secreted. Furthermore, the host's immune system response against bacteria results in an elevated wound temperature, as well as an up-expression of wound enzymes (e.g., lysozyme, protease, etc.) and signaling molecules (e.g., hydrogen peroxide (H_2O_2), nitric oxide, etc.)[45,46]. And more information about infection wound features can be found in these reviews[26,41,47,48].

## MXene-based flexible materials for infection wound detection

By leveraging these physical, chemical and biological properties of infected wound, many biosensors have been developed[49]. Among them, flexible material-based sensors are being vigorously investigated. The main strategy for constructing flexible sensors is to modify responsive materials or specific biomolecules on flexible electrodes to directly achieve the detection of physical, chemical or biological signals[50]. By using this strategy, many flexible sensors can effectively monitor alterations in the biomarkers of infected wounds. Compared with traditional detection methods, flexible wearable sensors can realize real-time quantitative monitoring, which can simplify sampling, shorten analysis time and reduce the dependence on empirical judgment[51]. Due to the low intervention toward patients, this strategy can greatly improve patient compliance, which is very necessary for the early detection of infected wounds[52]. However, the complex wound environment and low content biomarkers have significantly affected the detection performance of traditional detection methods[53]. At present, bacterial culture remains the gold standard for clinical diagnosis of bacterial

infection; however, it is less sensitive and may produce false negative results during the early stages of wound infection[54]. In contrast, flexible sensors leverage the characteristics of infected wounds to monitor real-time changes in wound parameters, providing valuable insights into whether the wound is infected. And the currently available MXene-based flexible materials for detecting infected wounds has been summarized in Table 1.

pH
The pH value in the infected tissue is different from normal tissue[55,56]. Thus, the measurement of pH value of an infected wound can provide insight into the healing process. Currently, Ti$_3$C$_2$T$_x$-based flexible and wearable pH sensors have been developed specifically for the detection of wound pH[57]. In this work, by electrostatic spinning strategy, polylactic acid/polyvinyl pyrrolidone (PLAP) fiber film with Kirigami structure was fabricated to endow the wound bandage with breathability, bendability, and stretchability. To confer the sterilizing effect, Ti$_3$C$_2$T$_x$ with photothermal antibacterial activity was modified to the upper layer of PLAP fiber film. To enable wound pH monitoring, polyaniline (PANI) and Ag/AgCl-modified thermoplastic polyurethane (TPU) fiber membranes was assembled and affixed to the underside of the PLAP fiber film. Among them, PANI and Ag/AgCl-modified membranes acted as the working and reference electrodes. By using this art bandage, the pH change caused by the bacterial infection could be monitored and the infected wound healed rapidly after the pathogens was removed by photothermal therapy. Similar to the Long's work, Kalasin et al. also employed PANI electrode as pH sensor[58]. In this flexible wearable sensor, a signal display accessory, controller unit, and inductor initiator can be found (Fig. 2a). Among them, the inductor initiator contained a pair of PANI/Cu$_2$O NPs-modified electrode, which can recognize the voltage distinction caused by the pH difference between the normal and wound

Fig. 2 | FLEX-AI wearable sensor for wound monitoring. a The structure and working principle of the FLEX-AI wearable sensor. **b** Anatomical view of bandage initiator. **c** Work concept of FLEX-AI wearable sensor. Reprinted with permission from ref. 58. Copyright 2022 American Chemical Society.
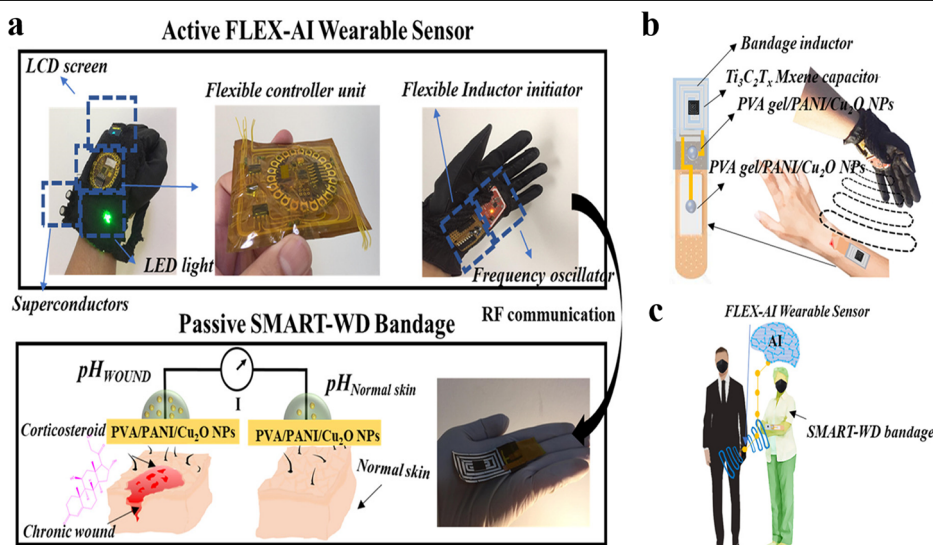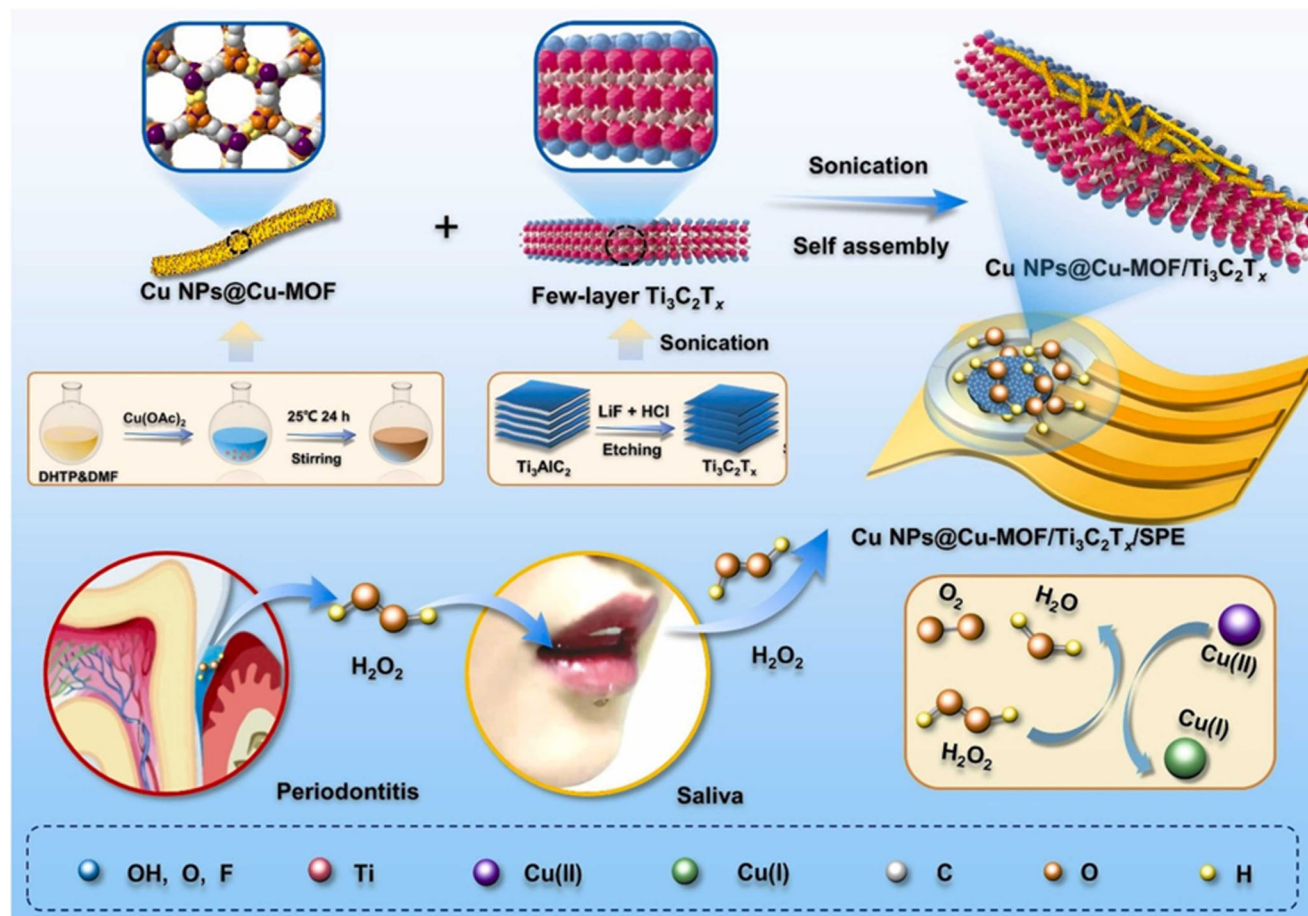
Fig. 3 | Cu NPs@Cu-MOF/Ti$_3$C$_2$T$_x$/SPE for the detection of H$_2$O$_2$ in patients with periodontitis. Reprinted with permission from ref. 62. Copyright 2023 Elsevier.

tissues. To implement portability and wearability, a Mxene capacitor, PANI-based pH sensors, and poly(vinyl alcohol) (PVA) adhesive were induced into the bandage (Fig. 2b). By combining artificial intelligence (AI) and PANI/Cu$_2$O NPs-based pH sensor, chronic wound healing progress can be read for supporting medical professionals in making decisions about treatment strategies and minimizing the incidence of wound infection (Fig. 2c).

H$_2$O$_2$

A high concentration of H$_2$O$_2$ was observed in the bacterial infected tissue[59–61]. By using abnormal H$_2$O$_2$ content, many responsive theranostic platforms have been developed[25]. However, few studies reported Ti$_3$C$_2$T$_x$-based flexible sensor for the detection of H$_2$O$_2$ in the infected tissue. Wang et al. developed a Cu NPs@Cu-MOF/Ti$_3$C$_2$T$_x$-modified flexible screen-printed electrode (SPE) for the detection of H$_2$O$_2$ (Fig. 3)[62]. The Cu NPs@Cu-MOF composites with the ability of electrochemical detection of H$_2$O$_2$ and Ti$_3$C$_2$T$_x$ with excellent electron transfer performance were modified into the surface of SPE electrode. Due to the synergistic interaction between Ti$_3$C$_2$T$_x$ and Cu NPs@Cu-MOF composites, Cu NPs@Cu-MOF/Ti$_3$C$_2$T$_x$/SPE present a distinguished selectivity, sensitivity (LOD: 84.5 nM), stability, and repeatability in the detection of H$_2$O$_2$. In actual clinical sample testing, the abnormal H$_2$O$_2$ content in the saliva and gingival crevicular fluid of patients with periodontitis can be detected for periodontitis diagnosis. Since the infected wound and periodontitis share similar pathological characteristics, for example, the H$_2$O$_2$ in the bacterial biofilm-infected tissues always exists at a relatively high level (~ 50-100 μM) owing to the high infiltration of immune cells surrounding infected tissues[63–65], thus this Cu NPs@Cu-MOF/Ti$_3$C$_2$T$_x$/SPE-based sensor can be used to detect open infected wounds by tracing H$_2$O$_2$ content by using electrochemical analysis technique.

Superoxide anion (O$_2^{\bullet-}$)

After bacterial infection, the immune cells (e.g., neutrophil and macrophage) can also synthesize and release O$_2^{\bullet-}$ to kill infectious pathogens[66,67]. Thus, O$_2^{\bullet-}$ can serve as a target for the detection of bacterial infection. However, in biological sample, O$_2^{\bullet-}$ is hard to be detect due to its low concentration and short life span. To achieve rapid and accurate detection of O$_2^{\bullet-}$, Li et al. used Mn$_3$(PO$_4$)$_2$ and Ti$_3$C$_2$T$_x$ MXene nanosheets to prepare a flexible sensing platform[68]. The strong interfacial interaction between Mn$_3$(PO$_4$)$_2$ and MXene nanosheets endows the Mn$_3$(PO$_4$)$_2$/MXene sensing platform with a superior flexibility while giving the Mn atom in the Mn$_3$(PO$_4$)$_2$/MXene with high energy state. Therefore, O$_2^{\bullet-}$ could be more easily adsorbed to the Mn$_3$(PO$_4$)$_2$ and oxidized by the Mn$_3$(PO$_4$)$_2$/MXene hybrid materials with the help of highly conductive MXene and the superoxide dismutase-like activity of Mn$_3$(PO$_4$)$_2$. The detection results showed that Mn$_3$(PO$_4$)$_2$/MXene/PE film electrode exhibited a low detection limit (1.63 nM), a broad linear operating range (5.75 nM-25.93 μM), and a high sensitivity (64.93 μA·μM^{-1}·cm^{-2}). Thanks to the above superior performance, Mn$_3$(PO$_4$)$_2$/MXene/PE film electrode could be used for the in-situ detection of O$_2^{\bullet-}$ that release by the cells. In the future, with appropriate modifications, we believe that this flexible sensing platform could be used for the detection of O$_2^{\bullet-}$ in infected wounds.

Temperature

After the wound is infected by the pathogens, the temperature of infected tissue will increase, which can use as an important parameter in the detection of wound infection[27]. Therefore, the development of MXene-based temperature sensor with high sensitivity in the human body temperature range can monitor the status of infected wounds in real time, which is helpful for medical staff to timely adjust the wound treatment strategy[69].
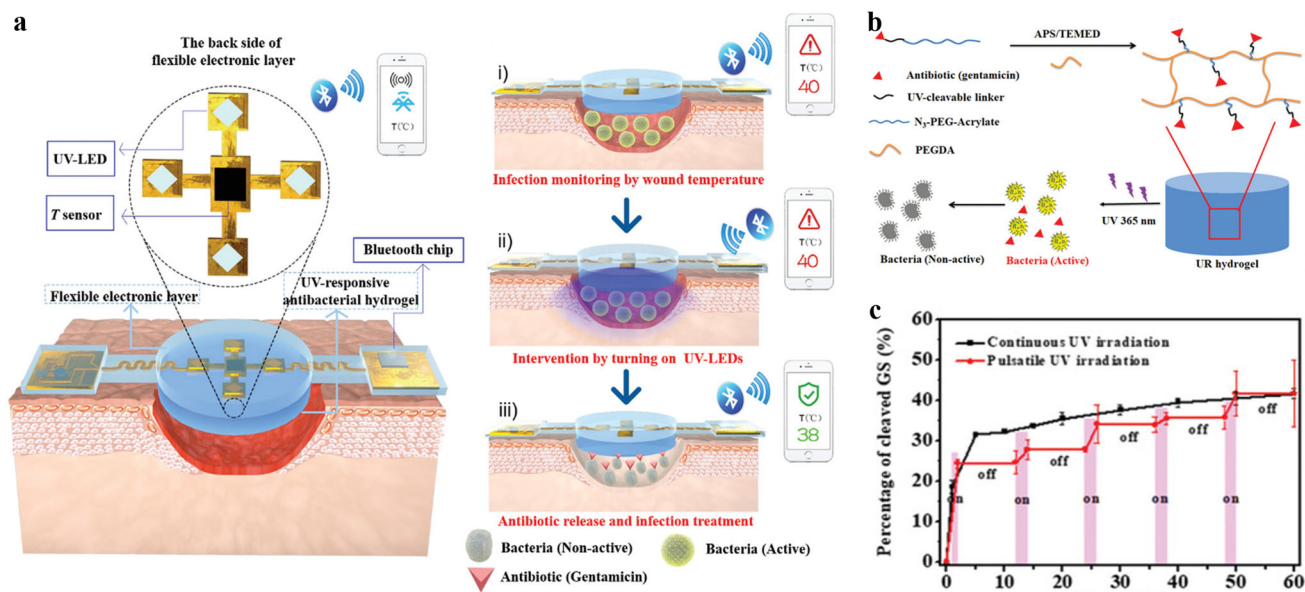
Fig. 4 | Temperature-responsive flexible electronic theranostic platform. a The structure and operation schematic of flexible wound dressing. In this system, PDMS-sealed flexible electronic superstratum includes UV-LEDs, temperature (T) sensor, a Bluetooth chip with immediate wireless signal delivery performance; UV-induced GS release hydrogel substratum was introduced for anti-infective therapy. (i-iii) Schematic diagram of working principle of theranostic dressing. (i) The wound temperature is measured in real time for offering high temperature warning caused by bacterial infection. (ii) switching on the UV-LEDs to activate the release of GS antibiotic. (iii) antibiotic release for bacterial removal, further reducing wound inflammation and wound temperature. **b** GS was modified to the PEG-based hydrogel via a UV-sensitive chemical bond. **c** GS release profiles under continuous (black line) and intermittent (red line, turn on 2 min /turn off 10 min for 5 circles) exposure to ultraviolet light. Reprinted with permission from ref. 69. Copyright 2022 Wiley-VCH GmbH.

For example, Pang and co-workers developed a wound dressing for precision treatment of infected wounds[69]. In this smart wound dressing, temperature sensor, UV-LEDs, Bluetooth chip, and UV-responsive hydrogel were integrated cleverly (Fig. 4a). Upon receiving a high temperature alert, UV-LEDs were turned on to trigger the release of gentamicin (GS) antibiotic due to the GS was conjugated into PEG-based hydrogel via an UV-sensitive nitrobenzyl linker (Fig. 4b). Then the released antibiotics could kill the bacteria at the infected site and reduce inflammatory response of wound. As a result, the temperature of the infected site would return to normal range. The experimental results showed that the temperature sensor integrated into flexible wound dressing could accurately and quickly measure the ambient temperature. In addition, the ultraviolet light emitted by UV-LEDs could significantly improve the release performance of antibiotics, to achieve accurate anti-wound infection treatment in mice (Fig. 4c).

Uric acid

Uric acid is involved in many vital processes in the body[70]. Previous evidences confirm that uric acid content in wound exudate is influenced by infectious pathogens. For example, a relatively low concentration of uric acid can be seen in *P. aeruginosa* and *S. aureus* infected wound as the uric acid can be hydrolyzed by microbial uricase[71]. Therefore, the monitoring of uric acid content in wounds can also evaluate the severity of bacterial infection[72].

To realize highly sensitive detection of uric acid, Chen et al. constructed an Au-Pd/$Ti_3C_2T_x$/laser scribed porous graphene (LSG) flexible sensors[73]. In this work, the designed electrode was printed on the polyimide (PI) film and treated with laser to prepare LSG electrode. Subsequently, the LSG electrode was modified with $Ti_3C_2T_x$ and Au-Pd metals to fabricate the final Au-Pd/$Ti_3C_2T_x$/LSR flexible electrode. The C-O-Ti covalent linkage between $Ti_3C_2T_x$ and LSG was conducive to the formation of two/three-dimensional hybrid framework. After that, using self-reducibility method, Au-Pd NPs was in situ grew on the $Ti_3C_2T_x$/LSR to enlarge its catalytic activity. In vitro analysis showed that Au-Pd/$Ti_3C_2T_x$/LSR flexible electrode with favorable electrochemical performances (e.g., high-stability, good reproducibility, and strong anti-interference) could be used for the detection of dopamine, ascorbic acid, and uric acid due to these biomolecules have specific oxidation peaks in the cyclic voltammetry test. Among them, the detection linear range of uric acid was 8 ~ 100 and 200 ~ 800 μM, the detection limit of Au-Pd/$Ti_3C_2T_x$/LSR for uric acid is 1.47 μM, which is much lower than the uric acid content (about 220 ~ 750 μM) in wound effluent[74]. As the smart bandage that developed by Wang' group for wound uric acid detection, Au-Pd/$Ti_3C_2T_x$/LSR flexible sensors could also be used for wound status analysis by tracing changes in uric acid concentrations in the future[71].

Bacterial virulence factors

During infection, the pathogens will secrete many kinds of virulence factors, which help bacteria colonize the site of infection and escape the clearance by the host immune system[75]. Thus, the virulence factors can serve as biomarkers for the detection of bacterial infection. For example, the sortase A from *S. aureus* has been used for the specific detection of pathogenic bacteria[76]. In addition, the bacterial toxin pyocyanin secreted by *P. aeruginosa* can also be used as a marker for the diagnosis of bacterial infection as pyocyanin possesses particular redox characteristics[77]. Based on the above research results, a flexible intelligent bandage sensor was constructed for the measurement of bacterial virulence factors, which can directly and instantaneously monitor wound infections (Fig. 5a, b)[78]. The flexible electrode pattern that included Ag/AgCl reference electrode, carbon counter electrode, and $Ti_3C_2T_x$-modified carbon electrode, was printed in a flexible PI film, cut and then enclosed in PDMS membrane (Fig. 5c). For the detection of sortase A, $Ti_3C_2T_x$-modified carbon electrode was further modified with ferrocenylacetic acid (Fc)-conjugate peptides (Fc-LPETGC) by Au-S bond, which can bind specifically to sortase A (Fig. 5d). For further convenience use, the flexible electrode array was assembled with near field communication (NFC) antenna, microcontroller unit, signal converter, and operational amplifier. And a porous cellulose membrane was integrated for the collection of wound exudates. The results obtained by differential pulse voltammetry showed that the resulting intelligent bandage has a linear
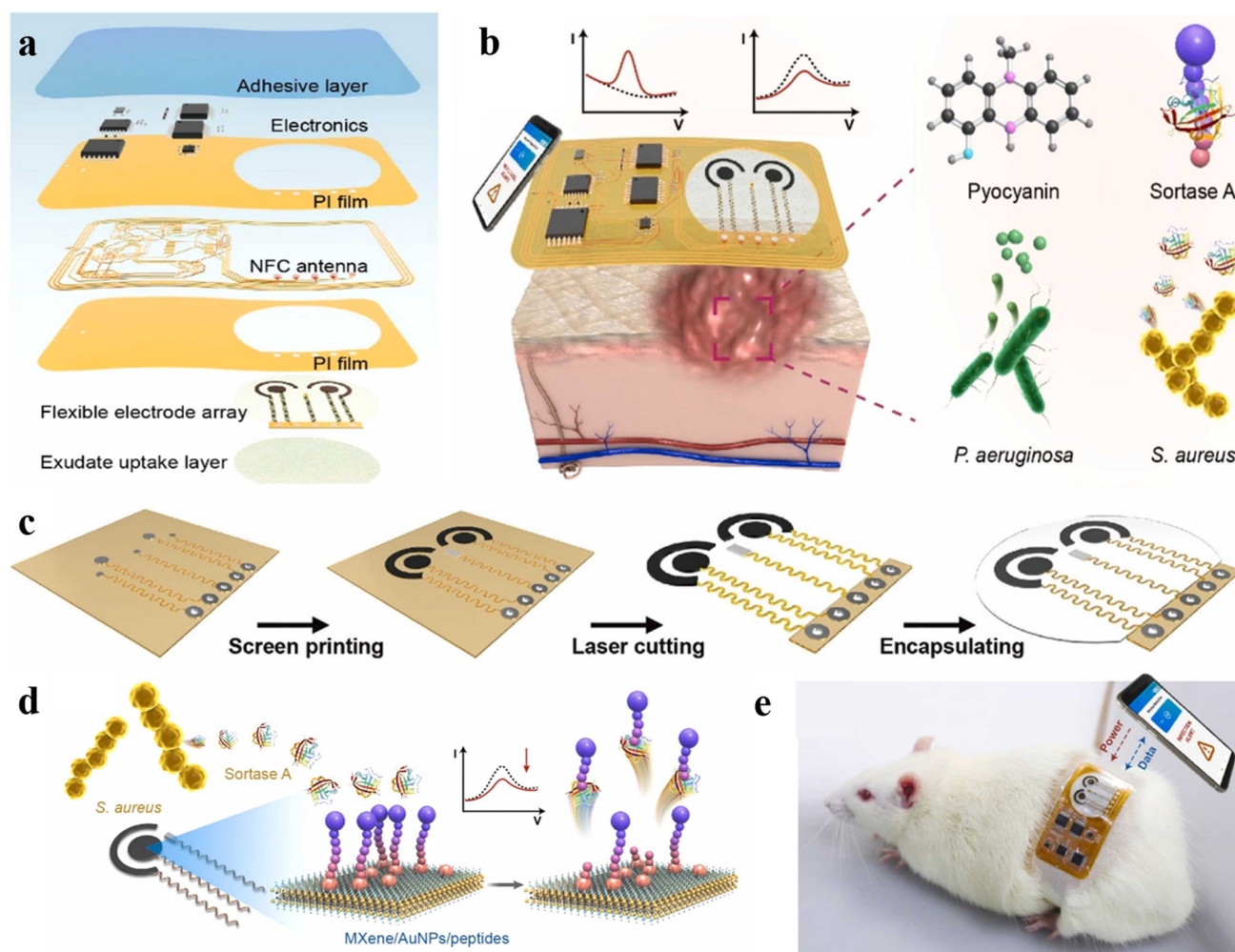
Fig. 5 | Smart bandage for the detection of bacterial toxin in the infected wound.
a Anatomical view of smart bandage. **b** Working mechanism of virulence factor detection by using smart bandage. **c** The preparation process of flexible electrode. **d** Electrochemical working process of MXene/AuNPS/peptides for the detection of sortase A. **e** Schematic diagram of wound virulence detection by using smart bandage. Reprinted with permission from ref. 78. Copyright 2023 Elsevier.

relationship in the range of 1 ~ 100 μM for pyocyanin and 1 ~ 100 ng/mL for sortase A, respectively. The mouse infection model showed that, with the aid of smartphones, the sensor data collection, analysis, and final detection results could be completed easily, which can be used for the detection of clinical wound infection (Fig. 5e).

Simultaneous detection of multiple parameters

Bacterial infections lead to changes in a variety of physiological parameters and biomarkers. To improve the accuracy of bacterial infection detection, simultaneous detection of multiple targets is favorable, which can effectively circumvent the generation of false positive signals. In addition, the sensors with multiple target detection performance can greatly reduce the sample demand and minimize the patient's discomfort[79]. Thus, the development of sensors with multicomponent detection function is extremely urgent.

To account for this, Park et al. developed smart flexible bandage with pH, uric acid, and temperature detection functions for chronic wound management (Fig. 6a)[80]. By using laser writing method, laser-guided graphene (LGG)-based circuit pattern was prepared after the PI film was irradiated with CO_2 laser. 2D MXene nanosheets were dripped onto the surface of three-dimensional (3D) porous LGG to synthesize LGG-MXene hybrid scaffolds. Then the electrode pattern was transferred on the PDMS flexible film and uric acid, pH, and temperature sensors were integrated into the LGG-MXene-based circuit and encapsulated with a transparent tape. Among them, uric acid sensor was composed of uricase (UOx)-modified

LGG-MXene working electrode (WE), LGG-MXene counter electrode (CE), and Ag/AgCl reference electrode (RE); the pH sensor was constructed by using PANI-functionalized LGG-MXene WE and Ag/AgCl RE; while LGG-MXene electrode was directly used as thermistor for the temperature detection. Using this integrated multifunctional flexible sensor, the pH value, uric acid concentration, and temperature in chronic wound could be detected rapidly and simultaneously, which offers a variety of precise physiological parameters that can serve as important references for the selection of treatment strategies for chronic wounds.

Using the electrode integration strategy, Park et al. also developed a butterfly-inspired hybrid epidermal biosensing (*bi*-HEB) flexible patches that can simultaneously detect temperature, pH, and glucose (Fig. 6b)[81]. To enhance the sensitivity and durability of *bi*-HEB sensor, $Ti_3C_2T_x$ MXene-modified nanoporous carbon (NPC@MXene) as transducing layer was introduced into the patch. To construct *bi*-HEB multifunctional sensor, the flexible PET film that deposits on the surface of silicon wafer is roughened by using O_2 plasma. Next, Pt coating as temperature sensor was laminated and treated with O_2 plasma. Afterward, Au was coated to the surface of the film according to the circuit diagram. Then SU-8 photoresist-passivated Pt-based temperature sensors was perforated with a CO_2 laser to increase air permeability. The butterfly-like electrode patch could be harvested after being cut and stripped away from the silicon wafer. In addition, to construct the WE of glucose sensor, platinum nanoparticles (PtNPs) and glucose oxidase (GOx) was successively modified to the surface of NPC@MXene. To
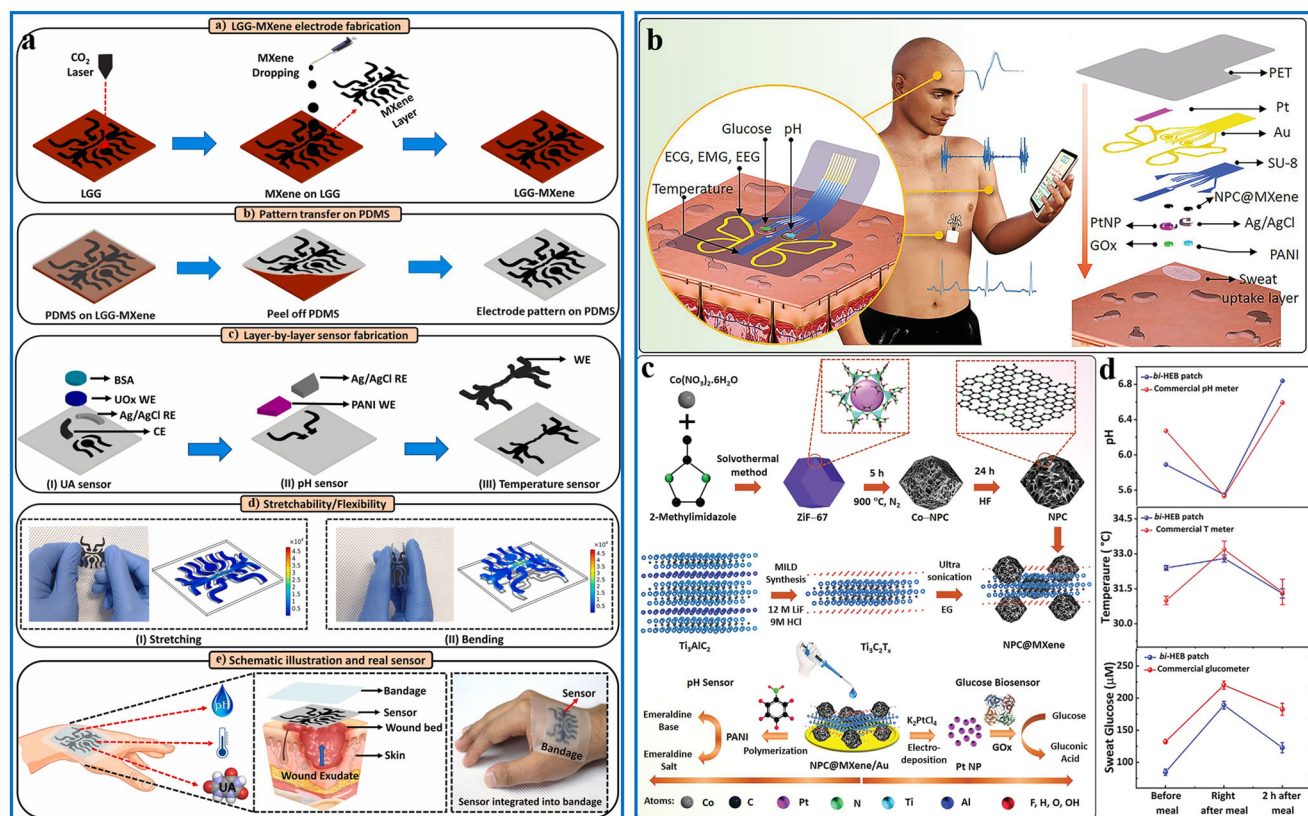
Fig. 6 | Flexible material for simultaneous detection of multiple parameters.
a The specific preparation process of stretchable and flexible smart bandage. Reprinted with permission from ref. 80. Copyright 2023 Elsevier. **b** bi-HEB patch was affixed to the chest for the detection of temperature, sweat glucose, sweat pH, and electrocardiogram (ECG). Anatomical view of flexible bi-HEB patch. Among these accessories, Butterfly-shaped wing was served as dry electrode for the detection of ECG/electroencephalogram (EEG)/electromyogram (EMG). The right picture shows the manufacture process of bi-HEB patch. Pt-based temperature sensor was

sealed with SU-8 photoresist. And all sensors were encapsulated in Nafion-based membrane. **c** The fabrication processes of pH and glucose sensors. Specifically, PANI-functionalized NPC@MXene/Au electrode was acted as pH sensor. PtNPs-modified NPC@MXene/Au electrode was served as electrocatalysts for glucose detection. **d** Sweat pH, human temperature, sweat glucose was monitored before and after meals by using bi-HEB patch and commercial sensors. Reprinted with permission from ref. 81. Copyright 2022 Wiley-VCH GmbH.

prepare the WE of pH sensor, aniline was polymerized in situ on the electrode surface (Fig. 6c). Finally, all sensors would be connected to a custom circuit board containing a microcontroller integrated Bluetooth Low-Energy module, electrocardiogram analog front end, and potentiostat to achieve wireless transmission of test results. In the epidermal assessments, the *bi*-HEB patch can quickly reflect the changing trend of temperature, pH value and glucose content in sweat in real time (Fig. 6d). However, the detection performance of *bi*-HEB flexible patches in infected wound still needs to be further investigated in future.

Infected wound management
Photothermal-mediated antimicrobial therapy
Among the multiple antibacterial treatments, photothermal therapy can effectively eradicate infectious pathogenic bacteria without inducing resistance[82,83]. $Ti_3C_2T_x$ with high photothermal conversion ability can kill the pathogens that locate in the infected tissue under the assistant of laser[36]. Currently, many $Ti_3C_2T_x$-based therapeutics have been developed for the management of infected wound. Among them, thin film-based therapeutic patches were widely used as it possesses elasticity, absorptive performance, and thinness, which facilitate absorb superfluous exudate, shield bacteria from invasion, kill infectious bacteria, and allow movement[84]. To construct the $Ti_3C_2T_x$-based film with antifouling and antibacterial functions, Wang et al. used perfluorosilane (PFOTS) to modify $Ti_3C_2T_x$ MXene to harvest superhydrophobic MXene nanosheets (MXene-F), which exhibited superior stability. Then 2,2,6,6-tetramethyl-1-piperidinyloxy-oxidized nanocellulose (TOCNF) and MXene-F were used for the construction of FMX-T composite

film by layer-by-layer self-assembly strategy. The introduction of TOCNF endowed FMX-T composite film with excellent flexibility and mechanical properties. During preparation, MXene-F was uniformly assembled on the membrane surface, which endow FMX-T film with photothermo-driven antibacterial properties, but also superhydrophobic property and high stability. Thus, MXene-F film serving as light-responsive flexible robot also can be used for the treatment of infected wound[85]. However, in the thin film-based treatment agents, it is commonly observed that the temperature of the upper layer is generally higher compared to the bottom layer. To overcome the problem of uneven heat distribution, Ding et al. employed micro-nano effect to efficiently transfer the heat generated from the upper surface to the bottom of fiber membrane. As a result, $Ti_3C_2T_x$-functionlized polylactic acid/gelatin-based fiber film could effectively remove infectious pathogens from the wound and effectively prevent infection recurrence[86].

In addition, to accelerate wound healing, the breathability of flexible wound dressing is very important for the oxygen supply. For that purpose, Wang et al. developed a breathable and flexible film (PMPP) by using $Ti_3C_2T_x$ MXene, PMDS, and polydopamine (PDA)-functionalized porous PU film for motion monitoring and photothermal inactivation of bacteria[87]. Taking advantage of the high conductivity of $Ti_3C_2T_x$, PMPP film exhibits a sensitive mechanical detection property as the film deformation will result in impedance increase. After PMPP film sensor was introduced into the insole and seat cushion, the human posture can be monitored and corrected, which may have potential in the detection and treatment of infected wound.

Compared with thin films, the hydrogels can absorb wound exudates, maintain an appropriate wound humidity, and has comparable mechanical

strength to biological tissue. By combining the advantages of the hydrogel with photothermal properties of $Ti_3C_2T_x$, a muscle-mimetic $Ti_3C_2T_x$ MXene/PVA hydrogel was developed for wound infection management[88]. Due to the existence of anisotropic and hierarchical structures, MXene@PVA exhibits favorable flexibility and plasticity, which could be used for wound protection. In addition, the interactive force between PVA and MXene allows the MXene to disperse evenly through the gel. After administration to infected wound, the MXene@PVA could effectively combat bacterial infection by photothermal antibacterial therapy with the aid of an 808 nm laser. These results confirmed that MXene@PVA hydrogel could serve as wound dressing to accelerate the healing of infected wound.

To enhance the effect of photothermal antibacterial therapy and reduce its damage to normal tissue, the combination of photothermal therapy and other treatments has attracted much attention[89]. Silver, as an efficient and ancient antibacterial agent, has been widely applied in the field of antibacterial[90]. For example, Zhong et al. embedded Ag nanoparticles (Ag NPs) and MXene-encapsulated $Fe_3O_4@SiO_2$ (MNPs@MXene) in a temperature-sensitive poly(N-isopropyl acrylamide)-alginate (NIPAM-Alg)-based double-network hydrogel (Fig. 7a)[91]. Under laser irradiation, the heat generated from MNPs@MXene induces the breakage of intramolecular hydrogen bonds of poly(N-isopropyl acrylamide), causing the shrinkage of hydrogel and the release of Ag NPs antibacterial agents. By using this smart MXene-based hydrogel system, the release of Ag NPs and photothermal therapy could be triggered for the treatment of chronic infected wound. In another studies, Ag NPs was in situ grew into the surface of $Ti_3C_2T_x$ to obtain MXene@Ag composite nanosheets. Due to the occurrence of localized surface plasmon resonance effects between Ag and MXene, MXene@Ag exhibits strong light capture ability and high photothermal conversion performance[92]. After sodium sulphate hydrated salts (SSD) phase change materials and MXene@Ag (MA) were embedded into a polyacrylamide (PAM)/sodium alginate (SA)-based hydrogel, the resulting PAM/SA/SSD/MA presents an excellent photothermal antibacterial and superior motion monitoring performance, which offers a wearable and flexible materials for human healthcare management.

The introduction of silver nanomaterials can not only improve the antibacterial properties of flexible wearable materials, but also increase their electrical conductivity and improve their own detection performance. For example, Wan et al. synthesized a breathable polyurethane-based (TPU/CS/MXene/AgNWs) elastomeric film sensors after TPU electrospinning film was modified with chitosan (CS), MXene, and silver nanowires (AgNWs) (Fig. 7b)[93]. The experimental results indicated that the resulting TPU/CS/MXene/AgNWs flexible electronic sensor features a favorable biocompatibility, high reliability, ultralow detection limit, high sensitivity (gauge factor up to 4720), and a wide detection range (up to ~120%), which could monitor many types of physiological signals (e.g., wrist bending, elbow bending and even blood pulse). In addition, due to the introduction of MXene and AgNWs, the TPU/CS/MXene/AgNWs wearable sensor also exerted excellent antibacterial activity by combined photothermal and silver antibacterial therapy upon exposure to 808 nm laser.

Aside from utilizing the inherent antibacterial properties of MXene, we can further incorporate additional antibacterial substances directly into MXene-based flexible dressings to effectively eliminate bacteria from infected wounds.

Accelerating wound closure

Accelerating wound healing by drug delivery. Ti_3C_2 MXene-based flexible material not only can directly inactivate pathogens via photothermal antibacterial therapy, but also can used for motion monitoring and the control of drug release due to its high conductivity and high photothermal conversion properties. By using the photothermal conversion properties of Ti_3C_2 MXene, Zhang and his coworkers synthesized a NIR light-triggered MXene nanobelt fibers after MXene nanosheets and vitamin E were embedded into the polyvinylpyrrolidone (PVP) and polyacrylonitrile (PAN) composite nanobelts by using electrospinning

technique. To achieve light-responsive release, a temperature-sensitive coating (P(AAm-co-AN-CO-VIm) copolymer, PAAV) was functionalized to the surface of nanobelts to obtain the final results. After administration to the wound, MXene-based nanobelts could release vitamin E for promoting wound healing under NIR laser irradiation. In addition, MXene-based nanobelts could contact with the skin and offer a favorable environment for cell growth and proliferation. Thus, MXene-based nanobelts could be used for accelerating wound closure[94]. However, due to the excessive inflammatory response at the wound site, the therapeutics with promoting would healing performance cannot effectively treat chronic wounds. To address this issue, Zhang subsequently developed an NIR laser-trigged MNFs@V-H@DA hybrid hydrogel for wound inflammation and revascularization regulation (Fig. 8a)[95]. In the fabrication process of MNFs@V-H@DA, vascular endothelial growth factor (VEGF)-loaded SiO_2 NPs and MXene nanosheets were firstly introduced into poly(lactide-co-glycolide) (PLGA) nanofibers to harvest MXene nanofibers@VEGF-loaded SiO_2 NPs (MNFs@V); Then dopamine-conjugated hyaluronic acid and diallyl trisulfide (DA) was coated on the surface of MNFs@V to synthesize dopamine-hyaluronic acid hydrogel (H) functionalized nanofibers (MNFs@V-H@DA). After MNFs@V-H@DA was applied to the wound, the release of VEGF could be controlled with the switch of an NIR laser; meanwhile, DA could be sustainably released from the MNFs@V-H@D hydrogel, which can generate H_2S to induce the formation of inflammatory M2 type macrophages. The in vivo evidences confirmed that MNFs@V-H@D could effectively promote wound healing while preventing fibrosis and scar formation by regulating wound immune reaction and vascularization. Therefore, MNFs@V-H@D could serve as band-aid for scarless wound healing and chronic wound treatment.

Microneedles (MNs) patches hold great application potential in wound treatment due to its painlessness, minimal invasion, and easy to multifunction and subcutaneous drug delivery. Based on this advantage, He et al. developed a cactus-inspired MXene-based hydrogel MNs for wound treatment (Fig. 8b)[96]. Firstly, MXene, spidroin (SR), PU solution, and aloe vera gel (avGel) mixture were used to print microneedle scaffold with inverse opal photonic crystal (IOPC) structure. Then the interstice of microneedle scaffold was filled with NIPAM solution that pre-added human epidermal growth factor (hEGF) and mupirocin antibiotic was induced to form a cross-linked network gel using an UV lamp. Under 808 nm laser irradiation, the heat generated by MXene could induce the deformation of NIPAM gel, further release the therapeutics (Fig. 8c). The in vivo test analysis showed that the final hydrogel MNs could be used for motion sensing by monitoring resistance changes. In addition, with NIR laser irradiation, the preloaded therapeutics (e.g., hEGF) and mupirocin bacteriostat could be released for expediting wound healing (Fig. 8d). In his team's follow-up study, an intestine-inspired hydrogel MNs was developed using similar strategy for wound treatment and motion sensing[97]. These results indicated that multifunction hydrogel MNs could serve as smart dressing for wound management.

Accelerating wound healing by using electrical stimulation. The open wounds are susceptible to bacterial infection, further resulting in delayed wound healing[1]. Thus, the development of MXene-based flexible material with antibacterial and healing properties is essential for wound healing. For example, Liu et al. constructed an PVA/MXene/PANI (PMP) hydrogel by two steps crosslinking method for wound management[98]. By using photothermal conversion performance of $Ti_3C_2T_x$-MXene and PANI, the pathogens in the wound could be eliminated upon receiving 808 nm laser irradiation. Meanwhile, the introduction of PANI and MXene endowed the PMP hydrogel with high conductivity. The biological activity measurement indicated that PMP hydrogel not only could enhance cell proliferation and migration in vitro under the stimulation of an applied electric field, but also speed wound healing by boosting revascularization and collagen deposition in vivo.
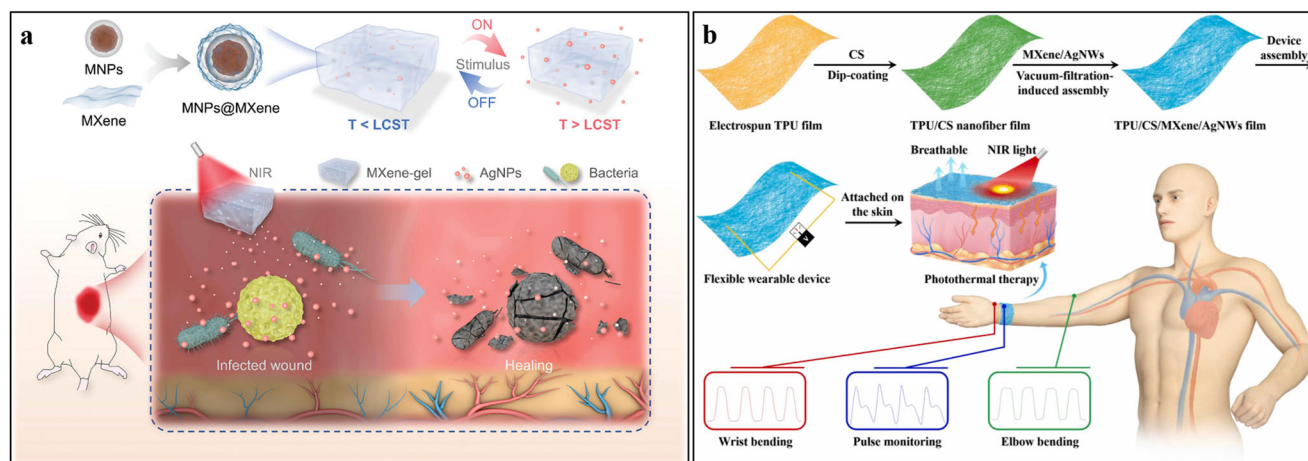
Fig. 7 | MXene-based dressings for photothermo-mediated antibacterial therapy. **a** Temperature-responsive MNPs@MXene and AgNPs-embeded NIPAM-Alg hydrogel for photothermo-induced AgNPs release and its application in AgNPs-assisted photothermal antibacterial therapy. Reprinted with permission from ref. 91. Copyright 2021 Wiley-VCH GmbH. **b** The fabrication process of TPU/CS/MXene/AgNWs elastomeric film and its application in healthcare monitoring and photothermal and silver combined antibacterial therapy. Reprinted with permission from ref. 93. Copyright 2023 Elsevier.
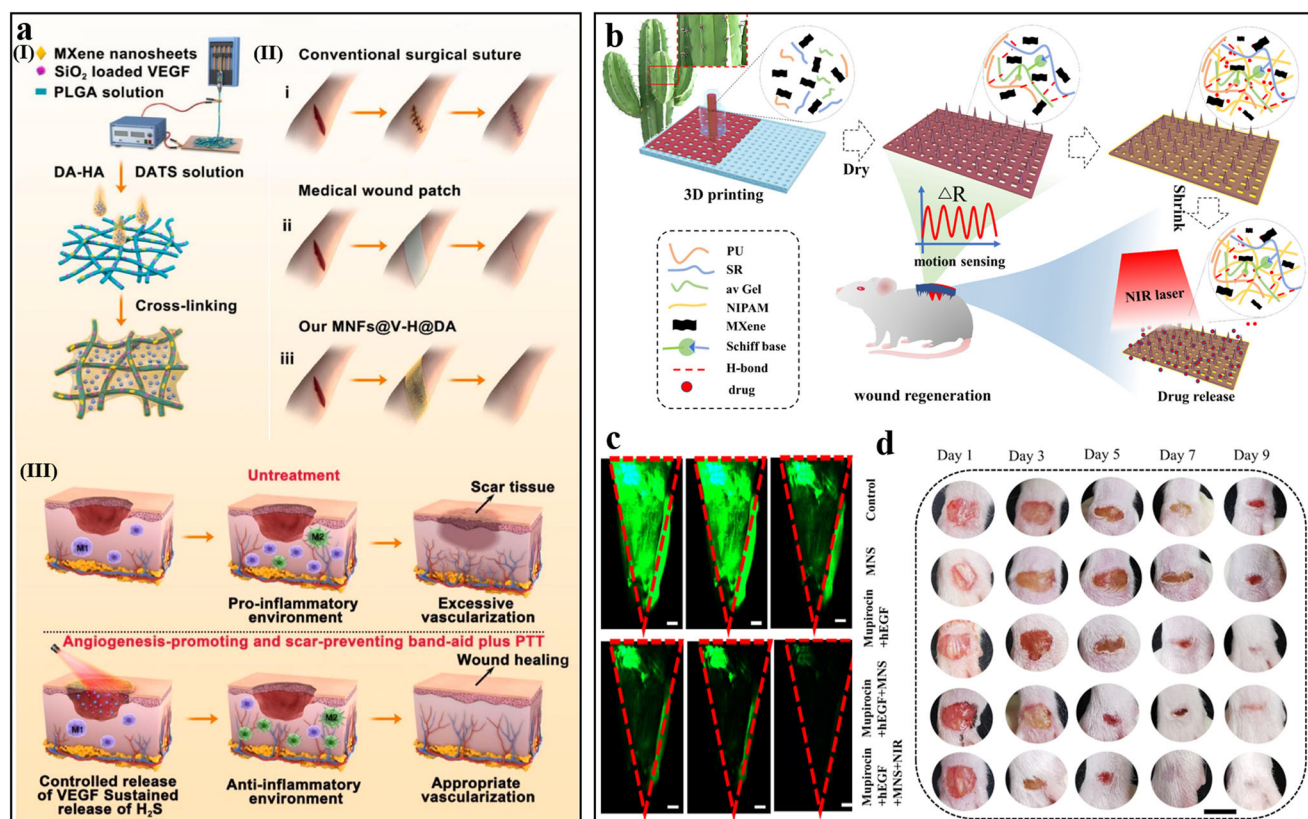

Fig. 8 | MXene-based hydrogel for accelerating wound healing by drug delivery. **a** (I) MNFs@V–H@DA hybrid hydrogel was prepared by using electrospinning and surface coating techniques. (II, III) MNFs@V–H@DA hydrogel for boosted wound healing and its action mechanism, respectively. Reprinted with permission from ref. 95. Copyright 2022 Elsevier. **b** Cactus-inspired MXene-based hydrogel MNs for motion detection and photothermo-triggered drug release. **c** The release behavior of loaded drugs (FITC-modified BSA). scale bar: 60 μm. **d** hEGF and mupirocin-loaded MNs for enhanced wound healing. scale bar: 500 mm. Reprinted with permission from ref. 96. Copyright 2022 American Chemical Society.

$Ti_3C_2T_x$-MXene can not only disrupt bacteria by photothermal therapy, but also kill bacteria by physical action due to the MXene nanosheets directly contact with pathogens and lead to bacterial membrane damage[17]. Since ultrathin $Ti_3C_2T_x$-MXene can exert antibacterial properties through the nanoknife effect. And corresponding antibacterial mechanism has been introduced systematically in the previous review[17]. Using this special physical properties of nanosheets, $Ti_3C_2T_x$-MXene doped poly (ε-caprolactone)/gelatin nanofibrous membranes (MPG NFMs) were prepared by Zhao et al. using electrospinning technique (Fig. 9a)[99]. MPG NFMs with high conductivity could mimic skin functions and respond to the electrophysiological signals of wound, which is beneficial for wound healing. By the combination of endogenous/exogenous electric fields and the bioactivity of
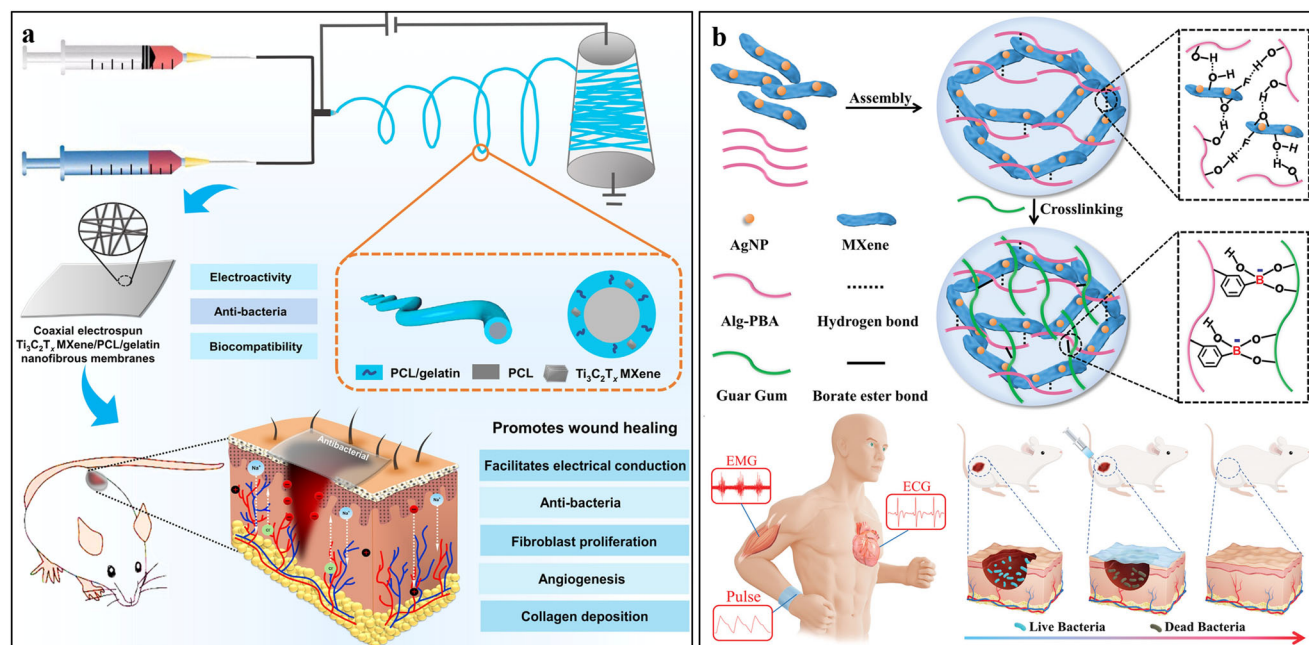
Fig. 9 | MXene-based flexible materials for accelerating wound healing by using electrical stimulation. a The synthesis process of MPG NFMs and its biologic activities in the treatment of infected wound. Reprinted with permission from ref. 99.

Copyright 2023 Tsinghua University Press. **b** The synthesis of AgNPs/MXene/GG/Alg-PBA hydrogel for physical health detection and infected wound treatment. Reprinted with permission from ref. 100. Copyright 2022 Wiley-VCH GmbH.

gelatin, MPG NFMs could obviously enhance wound healing by heightening cell adhesion, migration, and proliferation; besides, the MXene located in the surface of the MPG scaffold could effectually eliminate infectious pathogen through physical insertion effect. Meanwhile, $Ti_3C_2T_x$-MXene can function as an electroactive filler, further facilitating the reconstruction of endogenous electric fields. As a result, the treatment with MPG NFMs can effectively enhance the formation of granulation tissue, collagen, and blood vessels during wound healing. These results indicated that MPG NFMs as wound dressing could improve the outcome of wound treatment.

In addition to utilize the MXene's own antibacterial properties, other antibacterial agents can also be doped into MXene-based flexible material as described above. For example, Wan et al. developed a antibacterial hydrogel (Ag NPs/MXene/GG/Alg-PBA) for personal health diagnosis and wound treatment by direct introduction of Ag NPs-modified MXene nanosheets (Ag NPs/MXene) into the phenylboronic acid-conjected sodium alginate (Alg-PBA) and guar gum (GG)-based hydrogel (Fig. 9b)[100]. The Ag NPs make the hydrogel with superior antibacterial activity. In addition, the endogenous electric fields of wound could be reconstructed partly and a moist wound environment would be created after being treated with Ag NPs/MXene/GG/Alg-PBA hydrogel. As a result, infected wounds can heal rapidly. Moreover, the Ag NPs/MXene/GG/Alg-PBA could serve as epidermic sensor for motion and even electrophysiological signals monitoring. Therefore, the combination effect of electroactive material MXene and electrical stimulation offers an alternative strategy for accelerating wound healing[101].

To further verify the role of electrical stimulation in wound healing, Liu et al. fabricated a hydrogel-based bionic skin (CHHCMgel) by using CS, human-like collagen (HLC), hyperbranched polyglycidyl ether (HBPG), $Ti_3C_2T_x$ MXene, and graphene nanosheets as raw materials (Fig. 10a)[102]. Due to the existence of hydrogen, π-π, and amide bonds, the resulting CHHCMgel held superior self-healing and mechanical flexible performances. In addition, the properties of the raw materials and the gel itself endowed CHHCMgel with moisturizing, hemostatic, antibacterial, and conductive activities. After administration of CHHCMgel in vivo, the bacteria that locate in the infected wound could be inhibited, and the therapeutic effects and human motion (e.g., joint motion) could be

monitored by detecting the change of electrical resistance. Furthermore, with the addition of electrical stimulation, CHHCMgel could effectively transmit the exogenous electrical signal at the wound site, further promoting wound closure by expediting fibroblast and keratinocyte growth, collagen and granulation tissue formation, re-epithelization. Therefore, CHHCMgel offers a reference for the construction of flexible wound theranostic sensors.

Hemostasis
Some serious wounds are often accompanied by bleeding, which is not conducive to wound healing[103]. To achieve rapid wound healing, the therapeutics with hemostatic, anti-infective, and promoting wound healing activities are desperately needed.

Zhang and his group employed oxidized hyaluronic acid (H), poly(-glycerol-ethylenimine) (PE), PDA-functionalized $Ti_3C_2T_x$ nanosheets to construct HPEM hydrogel by using the Schiff-base reaction (Fig. 10b)[104]. HPEM hydrogel with self-healing behavior, tissue-adhesive ability, and electrical conductivity could promote rapid blood clotting, exert antibacterial performance via the cationic polyethylenimine (PEI). In addition, the PE bioactive molecules in the HPEM hydrogel could promote the MRSA-infected wound closure by inducing vascular endothelial differentiation and angiogenesis, enhancing cell proliferation, relieving inflammation, expediting collagen deposition and granulation tissue formation. Thus, multifunctional HPEM hydrogel has the potential to treat hemorrhagic infected wounds. In another studies, Cheng and coworkers synthesized polydopamine-modified $Ti_3C_2T_x$ MXene (MXene@PDA) for surface modification of CS non-woven fabric (Fig. 10c)[105]. The final product (M-CNF) held multiple biological functions (e.g., rapid hemostatic activity, strong antibacterial ability, and favorable biocompatibility). The antibacterial assay indicated that the bactericidal efficacy of 20 mg mL^{-1} MXene@PDA-modified M-CNF (M-CNF-20) toward E. coli and S. aureus reached 99.82% and 96.63%, respectively. The $Ti_3C_2T_x$ MXene with a large specific surface area and positively charged and microporous polysaccharide-based nanofiber film are benefit for platelets activation and blood coagulation. Thus, M-CNF-15 presented excellent hemostatic activity, which enabled to stop the bleeding within 48 s in a mouse model of liver bleeding. In addition, the electrical conduction function of M-CNF-15 to wound could facilitate wound closure as previously reported[106]. Pathological
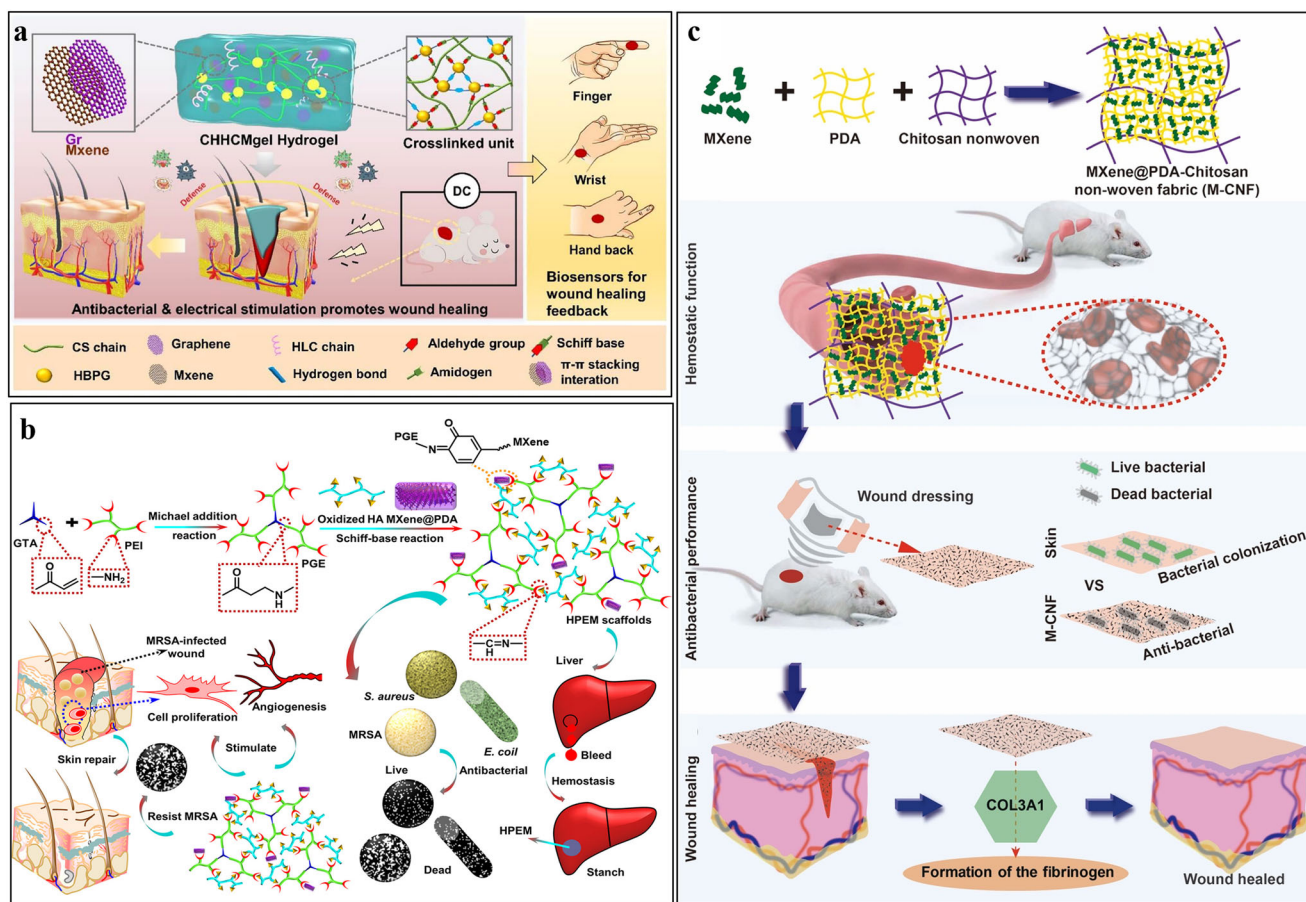
Fig. 10 | MXene-based flexible materials with hemostatic activity for the treatment of infected wounds. a Versatile CHHCMgel for health monitoring and wound treatment. Reprinted with permission from ref. 102. Copyright 2022 Elsevier. **b** HPEM hydrogel with antibacterial, hemostatic, and promoting performances for the treatment of bleeding and infected wound. Reprinted with permission from ref. 104. Copyright 2021 American Chemical Society. **c** The synthesis route of M-CNF and its application in the hemostasis, bacterial clearance, and wound healing. Reprinted with permission from ref. 105. Copyright 2022 Elsevier.

analysis results indicated that M-CNF-15 promoted wound healing by accelerating the fibrinogen and granulation tissue formation, which can be used for the treatment of bleeding-infected wounds.

Conclusions and prospects

Due to its special properties (e.g., conductivity, photophysical and nanoknife-like properties), MXenes display a wide application prospect in the fields of tumor treatment, biosensor, infection management, and wound healing etc. For example, MXene-involved flexible materials with detection or treatment performance have made important breakthroughs in the treatment of infected wound. The versatile functions of MXene-based flexible materials are mainly derived from their own its electrical, mechanical, physical, and chemical properties, which is vital for tissue regeneration, mechanical properties of biomimetic tissue, bioelectrical signal transmission, and the removal of exogenous invasive bacteria.

MXene-based flexible materials that have been developed so far exhibits favorable outcome in the detection and management of infected wounds. However, to achieve further industrialization and clinicalization, there are still several bottlenecks that need to be overcome.

Large quantities and high quality synthetic MXene

The synthesis of MXene is a prerequisite for their later application. Although several synthetic methods have been designed, some concerns still need attention because of the high risk of hydrofluoric acid (HF) used in the MXene-nanosheet stripping process. To overcome this issue, low concentration HF and salt-based etching approaches have been employed to synthesize high quality MXene nanosheets. Using the etching route, the yield of the MXene can be scaled up to the gram level. Moreover, by wet chemical etching, the production capacity can be boosted to kilograms or even tons just by scaling up the reaction system[107]. However, the effect of reaction solvent on properties and biosafety of MXene remains to be uncovered. In addition, how to formulate standard synthesis and assessment methods are crucial for quantitative and qualitative analysis of its biological activity, which is also essential for later clinical transformation of MXene-based flexible material in wound treatment. Another concern is that MXene will be oxidized under natural conditions, which is unfavorable for the stability of MXene-based flexible material. To relieve this issue, MXene is usually embedded in the polymer matrix to improve its oxidation stability during the synthesis of flexible materials.

Accurate and reliable detection of infected wounds

Few markers have been identified and used for the detection of infected wounds. The relationship between markers and wound infection degree was unclear and the internal relationship between the markers still needs to be further investigated. These situations indicate that the underlying pathological mechanism of wound infection needs further investigation. Nowadays, although some MXene-based flexible sensor with high sensitivity could be used for infected wound detection, the stability, repeatability, and reliability still need to be enhanced. In addition, MXene-based sensing unit also possess strong anti-interference ability and high signal-to-noise ratio. Therefore, the biophysical information that is harvested from sensors can really reflect idiographic circs, further facilitating medical workers to give the optimal treatment plan in time.

Skin adaptable flexible materials

Due to the irregular nature of the wound, MXene-based flexible materials should possess favorable flexibility and adaptability. Currently, MXene-based flexible materials can fit well to the wound even in the movement of the joints and exhibit superior biological activity. Owing to the mechanical and electrical properties of MXene, MXene-flexible materals have been used as a wound protective barrier while being conducive to the construction of endogenous electric field in the wound. Furthermore, these flexible materials should not cause detrimental effects to normal tissue during long-term usage. Despite abundant studies confirm the minor biotoxicity of MXene, more comprehensive and systematic biosafety should be performed before preclinical trials.

Integration of diagnosis and treatment

Most recent MXene-based flexible materials are constructed for detection or therapy. However, in general, the treatment of disease is inseparable from detection and therapeutics intervention. Therefore, the MXene-based flexible materials with both detection and therapeutic properties can achieve personalized precision therapy. To avoid false positives, multi-marker detection have been integrated into a single flexible material therapeutic platform due to the detection of multiple markers is conducive to the analysis of wound infection degree and treatment efficiency. In addition, based on the change of physiological and biochemical signals during infected wound treatment, responsive-therapeutic system can be carefully tailored. And the development of smart theranostic flexible material may be a fascinating and meaningful research direction in the future.

Clinical transformation

The establishment of dependable and scalable manufacturing techniques serves as the foundation for the eventual commercialization and clinical application of MXene-based flexible materials. Currently, numerous MXene-based flexible materials have demonstrated favorable properties in the detection and treatment of wound infections. However, the clinical application of these flexible materials is still in its early stages. The current experimental tests are primarily conducted under ideal conditions and do not account for the actual clinical environment[108]. Unlike previous conceptual studies, the clinical translation of flexible materials is a complex process involving scientific exploration, engineering transformation, clinical trials, and adherence to technical regulations. Moreover, medical materials are subject to strict regulations in most countries. Therefore, it necessitates cooperation among researchers, clinicians, and regulatory personnel to systematically investigate the clinical feasibility of flexible materials. Simultaneously, the establishment of a standardized test system for assessing the diagnostic accuracy and therapeutic performance of flexible materials is crucial for their future clinical implementation[109].

References

1. Hu, Y. et al. Stimuli-responsive therapeutic systems for the treatment of diabetic infected wounds. *Nanoscale* **14**, 12967–12983 (2022).
2. Zhou, S. et al. New insights into balancing wound healing and scarless skin repair. *J. Tissue Eng.* **14**, 20417314231185848 (2023).
3. Song, J. et al. Hydrogel-based flexible materials for diabetes diagnosis, treatment, and management. *npj Flex. Electron.* **5**, 26 (2021).
4. Dong, H. et al. Biofilm microenvironment response nanoplatform synergistically degrades biofilm structure and relieves hypoxia for efficient sonodynamic therapy. *Chem. Eng. J.* **453**, 139839 (2023).
5. Lv, X. et al. Recent nanotechnologies to overcome the bacterial biofilm matrix barriers. *Small* **19**, 2206220 (2023).
6. Lv, X. et al. Nitric oxide-assisted photodynamic therapy for enhanced penetration and hypoxic bacterial biofilm elimination. *Adv. Healthc. Mater.* **12**, 2302031 (2023).
7. Powers, J. G., Higham, C., Broussard, K. & Phillips, T. J. Wound healing and treating wounds: Chronic wound care and management. *J. Am. Acad. Dermatol.* **74**, 607–625 (2016).
8. Jiang, J. et al. Recent progress in nanozymes for the treatment of diabetic wound. *J. Mater. Chem. B* **11**, 6746–6761 (2023).
9. Tsegay, F., Elsherif, M. & Butt, H. Smart 3D printed hydrogel skin wound bandages: a review. *Polymers* **14**, 1012 (2022).
10. Ahmad, N. In vitro and in vivo characterization methods for evaluation of modern wound dressings. *Pharmaceutics* **15**, 42 (2023).
11. Zhang, Z. et al. Soft Bioelectronics for Therapeutics. *ACS Nano* **17**, 17634–17667 (2023).
12. Dong, R. & Guo, B. Smart wound dressings for wound healing. *Nano Today* **41**, 101290 (2021).
13. Kharaziha, M., Baidya, A. & Annabi, N. Rational design of immunomodulatory hydrogels for chronic wound healing. *Adv. Mater.* **33**, 2100176 (2021).
14. Yang, J., Jin, X., Liu, W. & Wang, W. A programmable oxygenation device facilitates oxygen generation and replenishment to promote wound healing. *Adv. Mater.* **35**, 2305819 (2023).
15. Lv, Y. et al. Multi-crosslinked hydrogels with strong wet adhesion, self-healing, antibacterial property, reactive oxygen species scavenging activity, and on-demand removability for seawater-immersed wound healing. *Acta Biomater.* **159**, 95–110 (2023).
16. Hu, Q. et al. Ultrathin, flexible, and piezoelectric Janus nanofibrous dressing for wound healing. *Sci. China Mater.* **66**, 3347–3360 (2023).
17. Seidi, F. et al. MXenes antibacterial properties and applications: a review and perspective. *Small* **19**, 2206716 (2023).
18. Al Mamun, A. et al. Oxygen releasing patches based on carbohydrate polymer and protein hydrogels for diabetic wound healing: A review. *Int. J. Biol. Macromol.* **250**, 126174 (2023).
19. Luo, R. et al. Reshaping the endogenous electric field to boost wound repair via electrogenerative dressing. *Adv. Mater.* **35**, 2208395 (2023).
20. Han, Z. et al. pH-Responsive wound dressings: advances and prospects. *Nanoscale Horiz.* **8**, 422–440 (2023).
21. Liang, Y., He, J. & Guo, B. Functional hydrogels as wound dressing to enhance wound healing. *ACS Nano* **15**, 12687–12722 (2021).
22. Wu, M. et al. Piezoelectric nanocomposites for sonodynamic bacterial elimination and wound healing. *Nano Today* **37**, 101104 (2021).
23. Jia, B. et al. Recent progress of antibacterial hydrogels in wound dressings. *Mater. Today Bio* **19**, 100582 (2023).
24. Mirani, B. et al. Smart dual-sensor wound dressing for monitoring cutaneous wounds. *Adv. Healthc. Mater.* **12**, 2203233 (2023).
25. Yang, S. et al. Stimuli-actuated turn-on theranostic nanoplatforms for imaging-guided antibacterial treatment. *Small* **19**, 2304127 (2023).
26. Tegl, G., Schiffer, D., Sigl, E., Heinzle, A. & Guebitz, G. M. Biomarkers for infection: enzymes, microbes, and metabolites. *Appl. Microbiol. Biotechnol.* **99**, 4595–4614 (2015).
27. Hu, Y. et al. Environment-responsive therapeutic platforms for the treatment of implant infection. *Adv. Healthc. Mater.* **12**, 2300985 (2023).
28. Darvishi, S. et al. Advances in the sensing and treatment of wound biofilms. *Angew. Chem. Int. Ed.* **61**, e202112218 (2022).
29. Saxena, S. et al. Nanotechnology Approaches for Rapid Detection and Theranostics of Antimicrobial Resistant Bacterial Infections. *ACS Biomater. Sci. Eng.* **8**, 2232–2257 (2022).
30. Li, Y., Shi, L., Cheng, Y., Wang, R. & Sun, J. Development of conductive materials and conductive networks for flexible force sensors. *Chem. Eng. J.* **455**, 140763 (2023).

31. Chen, X. et al. MXene/polymer nanocomposites: preparation, properties, and applications. *Polym. Rev.* **61**, 80–115 (2021).

32. Hermawan, A., Amrillah, T., Riapanitra, A., Ong, W.-J. & Yin, S. Prospects and challenges of mxenes as emerging sensing materials for flexible and wearable breath-based biomarker diagnosis. *Adv. Healthc. Mater.* **10**, 2100970 (2021).

33. Zhang, Y., Gong, M. & Wan, P. MXene hydrogel for wearable electronics. *Matter* **4**, 2655–2658 (2021).

34. Damiri, F. et al. MXene ($Ti_3C_2T_x$)-embedded nanocomposite hydrogels for biomedical applications: a review. *Materials* **15**, 1666 (2022).

35. Zhang, Y.-Z. et al. MXene hydrogels: fundamentals and applications. *Chem. Soc. Rev.* **49**, 7229–7251 (2020).

36. Fan, G. et al. MXene-based functional platforms for tumor therapy. *Adv. Mater.* **35**, e2302559 (2023).

37. Du, T. et al. MXene-based flexible sensors: materials, preparation, and applications. *Adv. Mater. Technol.* **8**, 2202029 (2022).

38. Wang, W., Ummartyotin, S. & Narain, R. Advances and challenges on hydrogels for wound dressing. *Curr. Opin. Biomed. Eng.* **26**, 100443 (2023).

39. Deng, Z., Yu, R. & Guo, B. Stimuli-responsive conductive hydrogels: design, properties, and applications. *Mater. Chem. Front.* **5**, 2092–2123 (2021).

40. Wang, X. et al. Mechanically robust, degradable and conductive MXene-composited gelatin organohydrogel with environmental stability and self-adhesiveness for multifunctional sensor. *Compos Part B-Eng.* **241**, 110052 (2022).

41. Pang, Q. et al. Smart wound dressing for advanced wound management: Real-time monitoring and on-demand treatment. *Mater. Des.* **229**, 111917 (2023).

42. Ren, Z. et al. Flexible Sensors Based on Organic–Inorganic Hybrid Materials. *Adv. Mater. Technol.* **6**, 2000889 (2021).

43. Sun, H. et al. Recent progress of intelligent antibacterial nanoplatforms for treating bacterial infection. *Chem. Eng. J.* **471**, 144597 (2023).

44. Wu, H.-J., Wang, A. H. J. & Jennings, M. P. Discovery of virulence factors of pathogenic bacteria. *Curr. Opin. Chem. Biol.* **12**, 93–101 (2008).

45. Zhang, J. et al. Recent design strategies for boosting chemodynamic therapy of bacterial infections. *Explor.* **4**, 20230087 (2024).

46. Xu, Y. et al. Environment-triggered nanoagent with programmed gas release performance for accelerating diabetic infected wound healing. *Chem. Eng. J.* **479**, 147645 (2024).

47. Wang, Z., Liu, X., Duan, Y. & Huang, Y. Infection microenvironment-related antibacterial nanotherapeutic strategies. *Biomaterials* **280**, 121249 (2022).

48. Mota, F. A. R., Pereira, S. A. P., Araújo, A. R. T. S., Passos, M. L. C. & Saraiva, M. L. M. F. S. Biomarkers in the diagnosis of wounds infection: An analytical perspective. *TrAC Trends Anal. Chem.* **143**, 116405 (2021).

49. Qureshi, A. & Niazi, J. H. Biosensors for detecting viral and bacterial infections using host biomarkers: a review. *Analyst* **145**, 7825–7848 (2020).

50. Han, S.-T. et al. An overview of the development of flexible sensors. *Adv. Mater.* **29**, 1700375 (2017).

51. Li, W.-D. et al. Recent advances in multiresponsive flexible sensors towards e-skin: a delicate design for versatile sensing. *Small* **18**, 2103734 (2022).

52. Sun, X. et al. A review of recent advances in flexible wearable sensors for wound detection based on optical and electrical sensing. *Biosensors* **12**, 10 (2022).

53. Lu, S.-H. et al. Multimodal sensing and therapeutic systems for wound healing and management: A review. *Sens. Actuators Rep.* **4**, 100075 (2022).

54. Li, K. et al. Vertical gold nanowires-based surface-enhanced Raman scattering for direct detection of ocular bacteria. *Sens. Actuat. B-Chem.* **380**, 133381 (2023).

55. Shi, Y. et al. An acidity-responsive polyoxometalate with inflammatory retention for NIR-II photothermal-enhanced chemodynamic antibacterial therapy. *Biomater. Sci.* **8**, 6093–6099 (2020).

56. Wu, J.-M., Liu, Y., Han, H.-Y. & Song, Z.-Y. Recent advances in endogenous and exogenous stimuli-responsive nanoplatforms for bacterial infection treatment. *Biomed. Eng. Commun.* **2**, 1–6 (2023).

57. Xu, L. et al. Stretchable, flexible and breathable polylactic acid/polyvinyl pyrrolidone bandage based on Kirigami for wounds monitoring and treatment. *Int. J. Biol. Macromol.* **237**, 124204 (2023).

58. Kalasin, S., Sangnuang, P. & Surareungchai, W. Intelligent wearable sensors interconnected with advanced wound dressing bandages for contactless chronic skin monitoring: artificial intelligence for predicting tissue regeneration. *Anal. Chem.* **94**, 6842–6852 (2022).

59. Li, X.-Y., Xiu, W.-J., Yang, D.-L. & Dong, H. Ultrasound-responsive microbubbles in antibacterial therapy. *Biomed. Eng. Commun.* **2**, 7–12 (2023).

60. Yang, N. et al. Infection microenvironment-activated nanoparticles for NIR-II photoacoustic imaging-guided photothermal/chemodynamic synergistic anti-infective therapy. *Biomaterials* **275**, 120918 (2021).

61. Wang, X. et al. Metformin capped $Cu_2(OH)_3Cl$ nanosheets for chemodynamic wound disinfection. *Nano Res* **16**, 3991–3997 (2023).

62. Wang, K. et al. Flexible screen-printed electrochemical platform to detect hydrogen peroxide for the indication of periodontal disease. *Sens. Actuat. B-Chem.* **390**, 133955 (2023).

63. Xu, Q. et al. A biofilm microenvironment-activated single-atom iron nanozyme with NIR-controllable nanocatalytic activities for synergetic bacteria-infected wound therapy. *Adv. Healthc. Mater.* **10**, 2101374 (2021).

64. Xiu W. et al. Biofilm microenvironment-responsive nanotheranostics for dual-mode imaging and hypoxia-relief-enhanced photodynamic therapy of bacterial infections. *Research*, 9426453 (2020).

65. Yang, D. et al. Nanotherapeutics with immunoregulatory functions for the treatment of bacterial infection. *Biomater. Res.* **27**, 73 (2023).

66. Grange, P. A. et al. Production of Superoxide Anions by Keratinocytes Initiates P. acnes-Induced Inflammation of the Skin. *PLoS Pathog.* **5**, e1000527 (2009).

67. Muniz-Junqueira, M. I. & de Paula-Coelho, V. N. Meglumine antimonate directly increases phagocytosis, superoxide anion and TNF-α production, but only via TNF-α it indirectly increases nitric oxide production by phagocytes of healthy individuals, in vitro. *Int. Immunopharmacol.* **8**, 1633–1638 (2008).

68. Zhao, S. F. et al. 2-D/2-D heterostructured biomimetic enzyme by interfacial assembling $Mn_3(PO_4)_2$ and MXene as a flexible platform for realtime sensitive sensing cell superoxide. *Nano Res* **14**, 879–886 (2021).

69. Pang, Q. et al. Smart Flexible Electronics-Integrated Wound Dressing for Real-Time Monitoring and On-Demand Treatment of Infected Wounds. *Adv. Sci.* **7**, 1902673 (2020).

70. El Ridi, R. & Tallima, H. Physiological functions and pathogenic potential of uric acid: A review. *J. Adv. Res.* **8**, 487–493 (2017).

71. Kassal, P. et al. Smart bandage with wireless connectivity for uric acid biosensing as an indicator of wound status. *Electrochem. commun.* **56**, 6–10 (2015).

72. Fernandez, M. L., Upton, Z., Edwards, H., Finlayson, K. & Shooter, G. K. Elevated uric acid correlates with wound severity. *Int. Wound J.* **9**, 139–149 (2012).

73. Wang, Y. et al. Self-reduction of bimetallic nanoparticles on flexible MXene-graphene electrodes for simultaneous detection of ascorbic acid, dopamine, and uric acid. *Microchem. J.* **185**, 108177 (2023).

74. Trengove, N. J., Langton, S. R. & Stacey, M. C. Biochemical analysis of wound fluid from nonhealing and healing chronic leg ulcers. *Wound Repair Regen.* **4**, 234–239 (1996).

75. Hu, Y. et al. Biofilm microenvironment-responsive nanoparticles for the treatment of bacterial infection. *Nano Today* **46**, 101602 (2022).

76. Tian, T. et al. Transpeptidation-mediated single-particle imaging assay for sensitive and specific detection of sortase with dark-field optical microscopy. *Biosens. Bioelectron.* **178**, 113003 (2021).

77. e Silva, R. F., Longo Cesar Paixão, T. R., Der Torossian Torres, M. & de Araujo, W. R. Simple and inexpensive electrochemical paper-based analytical device for sensitive detection of Pseudomonas aeruginosa. *Sens. Actuat. B-Chem.* **308**, 127669 (2020).

78. Shi, Z. et al. Wearable battery-free smart bandage with peptide functionalized biosensors based on MXene for bacterial wound infection detection. *Sens. Actuat. B-Chem.* **383**, 133598 (2023).

79. Xia, L.-Y., Tang, Y.-N., Zhang, J., Dong, T.-Y. & Zhou, R.-X. Advances in the dna nanotechnology for the cancer biomarkers analysis: attributes and applications. *Semin. Cancer Biol.* **86**, 1105–1119 (2022).

80. Sharifuzzaman, M. et al. Smart bandage with integrated multifunctional sensors based on MXene-functionalized porous graphene scaffold for chronic wound care management. *Biosens. Bioelectron.* **169**, 112637 (2020).

81. Zahed, M. A. et al. A Nanoporous Carbon-MXene Heterostructured nanocomposite-based epidermal patch for real-time biopotentials and sweat glucose monitoring. *Adv. Funct. Mater.* **32**, 2208344 (2022).

82. Lv, X. et al. An injectable and biodegradable hydrogel incorporated with photoregulated NO generators to heal MRSA-infected wounds. *Acta Biomater.* **146**, 107–118 (2022).

83. Yang, D. et al. Orthogonal Aza-BODIPY-BODIPY dyad as heavy-atom free photosensitizer for photo-initiated antibacterial therapy. *J. Innov. Opt. Health Sci.* **15**, 2250004 (2022).

84. Saraiva, M. M. et al. Alginate/polyvinyl alcohol films for wound healing: Advantages and challenges. *J. Biomed. Mater. Res. B* **111**, 220–233 (2023).

85. Tang, S. et al. Multifunctional sandwich-like composite film based on superhydrophobic MXene for self-cleaning, photodynamic and antimicrobial applications. *Chem. Eng. J.* **454**, 140457 (2023).

86. Ding, Y. et al. Mxene composite fibers with advanced thermal management for inhibiting tumor recurrence and accelerating wound healing. *Chem. Eng. J.* **459**, 141529 (2023).

87. Wang, X. et al. Biocompatible and breathable healthcare electronics with sensing performances and photothermal antibacterial effect for motion-detecting. *npj Flex. Electron.* **6**, 95 (2022).

88. Li, Y. et al. Muscle-inspired MXene/PVA hydrogel with high toughness and photothermal therapy for promoting bacteria-infected wound healing. *Biomater. Sci.* **10**, 1068–1082 (2022).

89. Yu, Q. et al. Near-infrared Aza-BODIPY Dyes through molecular surgery for enhanced photothermal and photodynamic antibacterial therapy. *Chem. Res. Chin. U.* **37**, 951–959 (2021).

90. Cao, C. et al. Mesoporous silica supported silver–bismuth nanoparticles as photothermal agents for skin infection synergistic antibacterial therapy. *Small* **16**, 2000436 (2020).

91. Yang, X. et al. Multiple stimuli-responsive MXene-based hydrogel as intelligent drug delivery carriers for deep chronic wound healing. *Small* **18**, 2104368 (2022).

92. Zhu, T.-y et al. MXene/Ag doped hydrated-salt hydrogels with excellent thermal/light energy storage, strain sensing and photothermal antibacterial performances for intelligent human healthcare. *Compos. Part A-Appl. S.* **170**, 107526 (2023).

93. Chao, M. et al. Flexible breathable photothermal-therapy epidermic sensor with MXene for ultrasensitive wearable human-machine interaction. *Nano Energy* **108**, 108201 (2023).

94. Jin, L. et al. NIR-responsive MXene nanobelts for wound healing. *NPG Asia Mater.* **13**, 24 (2021).

95. Jin, L. et al. An NIR photothermal-responsive hybrid hydrogel for enhanced wound healing. *Bioact. Mater.* **16**, 162–172 (2022).

96. Shao, Y., Dong, K., Lu, X., Gao, B. & He, B. Bioinspired 3D-printed mxene and spidroin-based near-infrared light-responsive microneedle scaffolds for efficient wound management. *ACS Appl. Mater. Interfaces* **14**, 56525–56534 (2022).

97. Lu, H., Shao, W., Gao, B., Zheng, S. & He, B. Intestine-inspired wrinkled MXene microneedle dressings for smart wound management. *Acta Biomater.* **159**, 201–210 (2023).

98. Liu, S. et al. Flexible, high-strength and multifunctional polyvinyl alcohol/MXene/polyaniline hydrogel enhancing skin wound healing. *Biomater. Sci.* **10**, 3585–3596 (2022).

99. Xu, S. et al. Electroactive and antibacterial wound dressings based on $Ti_3C_2T_x$ MXene/poly(ε-caprolactone)/gelatin coaxial electrospun nanofibrous membranes. *Nano Res* **16**, 9672–9687 (2023).

100. Li, M. et al. Flexible accelerated-wound-healing antibacterial mxene-based epidermic sensor for intelligent wearable human-machine interaction. *Adv. Funct. Mater.* **32**, 2208141 (2022).

101. Li, S. et al. MXene-Enhanced Chitin Composite Sponges with Antibacterial and Hemostatic Activity for Wound Healing. *Adv. Healthc. Mater.* **11**, 2102367 (2022).

102. Luo, X. et al. Tissue-nanoengineered hyperbranched polymer based multifunctional hydrogels as flexible "wounped treatment-health monitoring" bioelectronic implant. *Appl. Mater. Today* **29**, 101576 (2022).

103. Cao, C. et al. Biodegradable hydrogel with thermo-response and hemostatic effect for photothermal enhanced anti-infective therapy. *Nano Today* **39**, 101165 (2021).

104. Zhou, L. et al. Conductive Antibacterial Hemostatic Multifunctional Scaffolds Based on $Ti_3C_2T_x$ MXene Nanosheets for Promoting Multidrug-Resistant Bacteria-Infected Wound Healing. *ACS Nano* **15**, 2468–2480 (2021).

105. Li, H., Dai, J., Yi, X. & Cheng, F. Generation of cost-effective MXene@polydopamine-decorated chitosan nanofibrous wound dressing for promoting wound healing. *Biomater. Adv.* **140**, 213055 (2022).

106. Snyder, A. R., Perotti, A. L., Lam, K. C. & Bay, R. C. The influence of high-voltage electrical stimulation on edema formation after acute injury: a systematic review. *J. Sport Rehabil.* **19**, 436–451 (2010).

107. Ahmed, A. et al. Two-dimensional MXenes: New frontier of wearable and flexible electronics. *InfoMat* **4**, e12295 (2022).

108. Chen, K., Ren, J., Chen, C., Xu, W. & Zhang, S. Safety and effectiveness evaluation of flexible electronic materials for next generation wearable and implantable medical devices. *Nano Today* **35**, 100939 (2020).

109. Zhang, T. et al. Flexible electronics for cardiovascular healthcare monitoring. *Innovation* **4**, 100485 (2023).

Acknowledgements

Author contributions

Y.L.H. and D.L.Y. wrote original draft. H.Y. and J.G.J. contributed to paper writing. S.K.L, B.Y.D., J.H.L., J.Y., X.J.S. and J.J.Z conceptualized,

investigated, and wrote original draft, L.G., Y.N.X. and D.L.Y. conceptualized, supervised, and edited draft. All authors participated in scientific discussion. Y.L.H. and F.F.W. are co-first authors.

Competing interests
The authors declare no competing interest.

Additional information
Correspondence and requests for materials should be addressed to Yannan Xie, Li Gao or Dongliang Yang.

Reprints and permissions information is available at http://www.nature.com/reprints

Publisher's note Springer Nature remains neutral with regard to jurisdictional claims in published maps and institutional affiliations.